General Approach for Accurate Evaluation of Transformer Resonance Effects

M. Popov

Abstract- **In this paper, resonance effects in transformer windings are thoroughly investigated and analyzed. The resonance is determined by making use of an accurate approach based on the application of the impedance matrix of a transformer winding. The method is validated by a test coil and the numerical results are verified by an ATP-EMTP model. Further analysis is applied on a transformer winding for which the inductance and the capacitance matrix as well as the winding losses are previously determined. By having determined the amplification factor, it can be found the location where the most severe transients may occur. It is also shown that maximum resonance overvoltage depends on the duration of the excitation and its resonance frequency.**

Keywords: **Resonance, overvoltages, transformer winding, voltage distribution, amplification factor.**

I. INTRODUCTION

TRANSFORMERS are important devices which are inevitable for the existence and the operation of power systems. The study of transient behavior of transformer voltages and currents is important for transformer designers and system planners, in order to know the interaction between the transformer and the system during different disturbances. Transformers may normally possess more resonance (natural) frequencies, which exist because transformer windings and coils can be seen as a number of series inductances and shunt capacitances. When a transformer is excited by a voltage that oscillates with a frequency equal to some of the resonance frequencies, a resonance occurs. During this process, the total winding impedance is determined by the coper losses of the transformer winding. Hence, the resonance is a phenomenon in which the terminal transformer impedance is fully resistive and the imaginary impedance part is equal to zero. In this case, the total impedance becomes either minimum (series resonance) or maximum (parallel or anti-resonance). In case of a series resonance, the transformer is exposed to high overvoltages voltages, and the voltage distribution in the winding is non-linear since winding capacitances cannot be ignored. The evaluation of this distribution is important in order to know, which of the windings experience the highest stresses and under which conditions; lightning or switching. One important parameter that provides insight about voltage amplitudes along the winding is the *amplification factor*. This parameter was studied in [1]. During non-standard waves, resonance overvoltages may take different values. The analysis is performed to a single transformer even though the procedure is valid for multi- transformer windings as long as the impedance matrices, the elements of which are frequency dependent, are accurately determined.

Nowadays different types of models are applied to study transformer transients. The powerful vector fitting model, which is very accurate belongs to the group of blackbox modeling [2]. Its application depends on the measured admittance matrices within broad frequency range. A model based on 2 port network representation by making use of a Frequency Response Analysis (FRA) is another example of an efficient black box approach [3]. Another types of models are white box models. These are numerical models that make use of inductance-, capacitance- and resistance matrices. The advantage of the white box models is that transient analysis is performed within broad frequency range. However, the disadvantage is that the accuracy strongly depends on the accuracy of computed parameters, particularly inductance and capacitance matrix as well as losses, which are frequency dependent [4], [5], [6]. Finally, the last types of models are gray box models. These models are built in EMTP-based software packages, and some transformer parameters previously determined by white box model can be tuned to the measured values (black-box). In this way, inaccuracies of white box model can be eliminated.

In this work, an accurate modeling of the transformer winding based on the nodal admittance matrix is presented. Firstly, the modeling approach is described and applied to a transformer winding for which the parameters are known. Besides, the C-, L- and R-matrices are with constant parameters, so the model can also be implemented in ATP-EMTP environment and verified by a numerical analysis. Thereafter, a detailed analysis is performed on a foil-type transformer [4].

The paper is organized as follows. Section II explains the computational procedure. Section III deals with the verification of the model by an EMTP model; white box model is verified by EMTP simulations. In Section IV, a detailed analysis of a transformer winding for which the parameters are known is performed. Section V and Section VI deal with the discussion of the results and conclusion respectively.

II. COMPUTATION STRATEGY

According to [1], the transformer is fully determined when the $\underline{Z}$ matrix of the transformer winding is known. The voltages and currents can be computed by making use of:

M. Popov is with the Delft University of Technology, Faculty of EEMCS, Mekelweg 4, 2628CD, Delft, The Netherlands (e-mail: m.popov@ieee.org).

$$\underline{\mathbf{I}} = \underline{\mathbf{Y}}\underline{\mathbf{U}} \qquad (1)$$

in which, $\underline{\mathbf{I}}$ is a vector of current injections in the coil/turns, $\underline{\mathbf{Y}}$ is a square admittance matrix of the winding and $\underline{\mathbf{U}}$ is a vector of voltages to ground at each coil/turn. Matrix $\underline{\mathbf{Y}}$ is defined as:

$$\underline{\mathbf{Y}} = \frac{\mathbf{\Gamma}}{s} + \mathbf{G} + s\mathbf{C} \qquad (2)$$

where $\mathbf{G}$ is the matrix of conductances, $\mathbf{C}$ is the matrix of capacitances and $\mathbf{\Gamma}$ is the nodal inductance matrix, which also takes into account series losses. In general, it may take into account frequency dependent self- and mutual inductances, and frequency dependent losses including proximity effects as well. Since the accuracy of the computed voltages is highly dependent on the accuracy of the parameters, it is important to investigate how accurate the input parameters are and what the frequency range of model application is. $\underline{\mathbf{Z}}$ matrix can be obtained by inversion of $\underline{\mathbf{Y}}$. In this way, the relation between voltages represented in vector $\underline{\mathbf{U}}$ and currents in vector $\underline{\mathbf{I}}$, can be represented as:

$$\underline{\mathbf{U}} = \underline{\mathbf{Z}}\underline{\mathbf{I}} \qquad (3)$$

When j-th coil is excited by current i_j, the coil voltages can be found as:

$$
\begin{bmatrix} u_1 \\ u_2 \\ . \\ u_j \\ . \\ u_n \end{bmatrix} =
\begin{bmatrix}
Z_{11} & Z_{12} & Z_{13} & .... & Z_{1n} \\
Z_{21} & Z_{22} & Z_{23} & .... & Z_{2n} \\
. & & & & \\
Z_{j1} & Z_{j2} & Z_{j3} & .... & Z_{jn} \\
... & & & & \\
Z_{n1} & Z_{n2} & Z_{n3} & .... & Z_{nn}
\end{bmatrix}
\begin{bmatrix} i_1 \\ 0 \\ . \\ 0 \\ . \\ 0 \end{bmatrix} \qquad (4)
$$

It is easy to show that when a current is injected in the sending end of the winding, the ratio between the voltage drop of an arbitrary coil point j and the terminal voltage with respect to the terminal voltage can be represented as:

$$Amp = \frac{u_1(j\omega) - u_j(j\omega)}{u_1(j\omega)} = \frac{Z_{11}(j\omega) - Z_{j1}(j\omega)}{Z_{11}(j\omega)} \qquad (5)$$

Equation (5) is known as an amplification factor. When the source voltage u_1 is also known, the voltage at each coil u_j can be determined by:

$$u_j(j\omega) = \frac{z_{j1}(j\omega)}{z_{11}(j\omega)} u_1(j\omega) \qquad (6)$$

The time domain voltage distribution can be calculated by making use of inverse Modified Fourier Transform, or other techniques like inverse FFT, inverse Laplace or convolution. In this work, the time domain solution is provided by:

$$u_j(t) = \frac{1}{2\pi} \int_{-\Omega}^{\Omega} \frac{\sin(\pi\omega/\Omega)}{\pi\omega/\Omega} u_j(b + j\omega)e^{(b + j\omega)} d\omega \qquad (7)$$

If we divide the real and imaginary part of the integral function, and if we apply the property of evenness of the real part and oddness of the imaginary part with respect to ω, the following expression can be used [7]:

$$u_j(t) = \frac{2e^{bt}}{\pi} \int_{0}^{\Omega} \frac{\sin(\pi\omega/\Omega)}{\pi\omega/\Omega} real\{u_j(b + j\omega)\}\cos(\omega t)d\omega \qquad (8)$$

In (8), the interval $[0, \Omega]$, the smoothing constant b and the step frequency length $d\omega$ must be chosen properly in order to arrive at an accurate time-domain response. The modified transformation requires the input function $u_j(\omega)$ to be filtered by an $\exp(-bt)$ window function. To compute the voltages in separate coils the same procedure can be applied.

III. MODEL VERIFICATION

The described procedure in the previous section is applied on a test transformer for which the parameters of the coils and explanation of how the matrices are built are provided in the Appendix I. These parameters are taken from a test coil, the measurements of which are also shown in [1]. These data are also used for the EMTP model as shown in Figure 1. The $\mathbf{L}$ matrix with mutual inductances among all inductive elements is not seen in this figure.
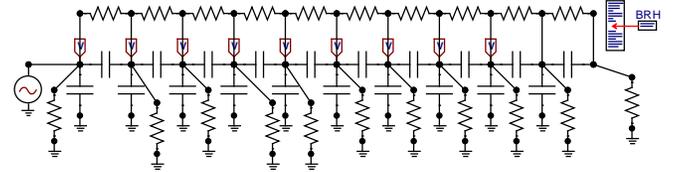
Figure 1. An illustration of the test circuit.

Figure 2 shows a comparison of the harmonic terminal impedance of the numerical model and EMTP model. Amplitude and phase characteristics are compared and it can be seen that both are in good agreement. The advantage of this implementation is that it offers possibility to observe the interaction of the transformer with a specific network.

(Anti)resonances occur whenever for some particular frequency, harmonic impedance phase angle is zero. Figure 3 represents the computed amplification factors for the observed frequency spectrum. It can be seen that maximum amplification factors for all coils occur at resonance frequency of 7.4 kHz. At this frequency, the phase changes its sign from negative to positive (from predominantly capacitive to predominantly inductive). It can also be seen that the amplification factors for different coils are different. In this case the highest amplification occurs in coil 6.
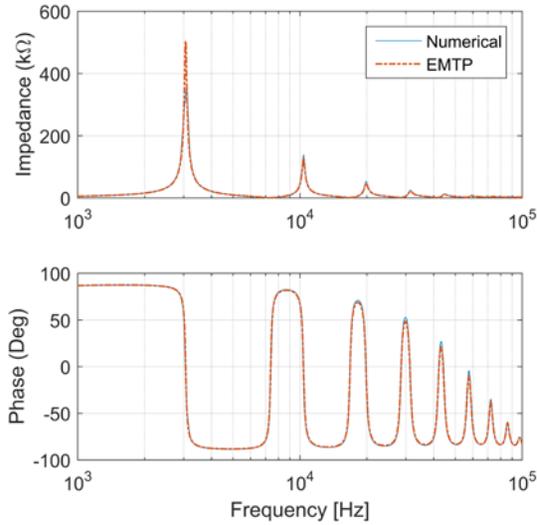
Figure 2. Comparison between numerical computation and simulation of harmonic terminal amplitude impedance (upper graph) and phase impedance (lower graph).
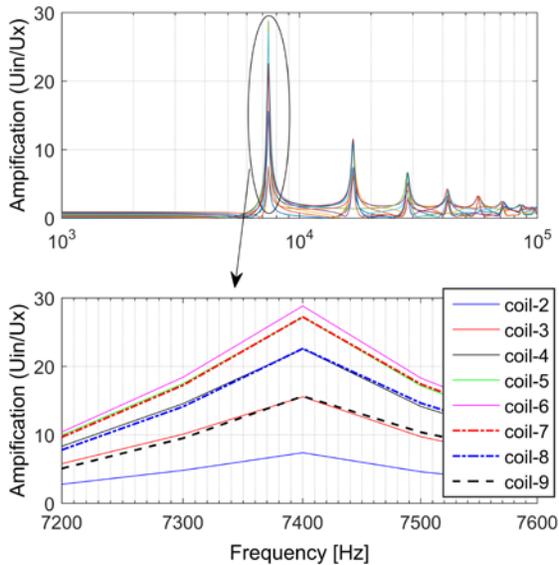
Figure 3. Computed amplification factors for all coils for the observed frequency spectrum (upper graph); increased time scale of the amplification factors around resonance frequency of 7.4 kHz.
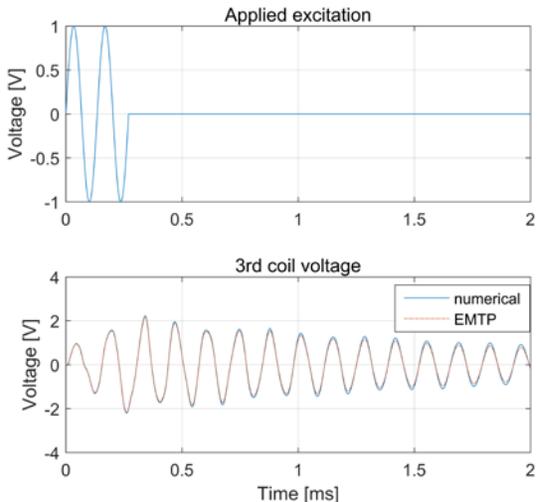
Figure 4. Applied excitation and voltage response in the 3rd coil.
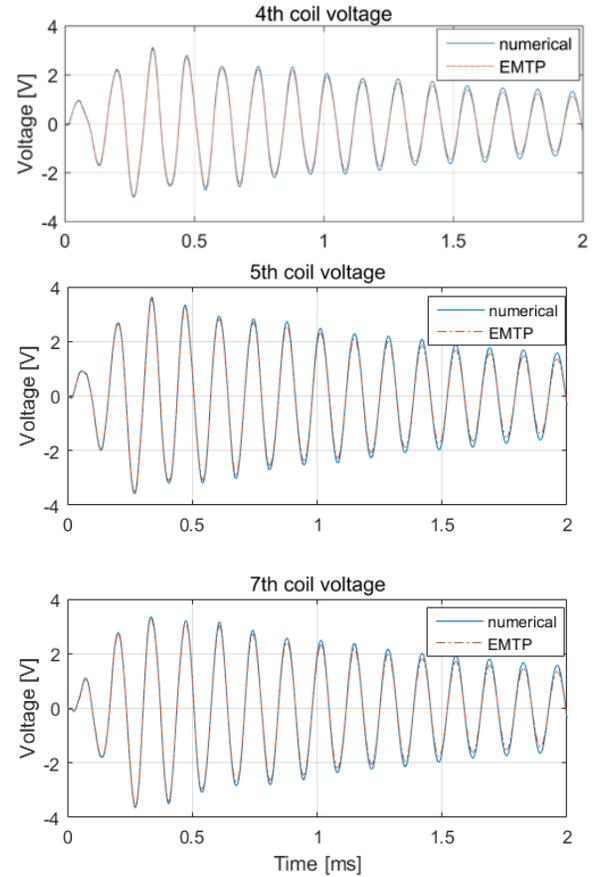
Figure 5. Voltage oscillation in coils 4, 5 and 7 upon an excitation as shown in Figure 4.

The verification of the model is demonstrated by applying a sinusoidal pulse with a duration of two periods and a frequency equal to 7.4 kHz, which is the most severe resonance frequency for this transformer. Figure 4 shows the applied excitation and the voltage response in coil 3. It is evident to see the occurrence of resonance in these figures since the voltage increases in magnitude and thereafter gradually decreases. It is also evident that the voltage in different coils rises above the excitation voltage amplitude.

IV. DETAILED ANALYSIS OF A TRANSFORMER WINDING

In this section, a detailed analysis of a transformer winding is presented. The parameters of an actual foil-type transformer winding including can be found in [4]. Further analysis on the parameters is beyond the scope of this work. The transformer winding consists of 13 coils, and the model is applied only on coils and not on turn and interturn voltages, even though this is also possible, if detailed representation of the **L**-,**C**- and **R**-matrices of the coils are known. This can be done in two steps as it is explained in [6].

Figure 6 shows the harmonic terminal impedance of the studied transformer. This is a simulated characteristic and it is in a good agreement with the measurements provided in [4,8]. It can be seen that this transformer has several resonance frequencies. The denoted resonance frequency (36.8 kHz) is the one that results in the highest amplification factor. Figure 7 shows the amplification factors in transformer coils during

resonance that results from this oscillation frequency. Coil 7 is the one exposed to highest overvoltage that is about 9 pu. Amplification factors gradually decrease from coil 7 toward the remote ends of the winding.
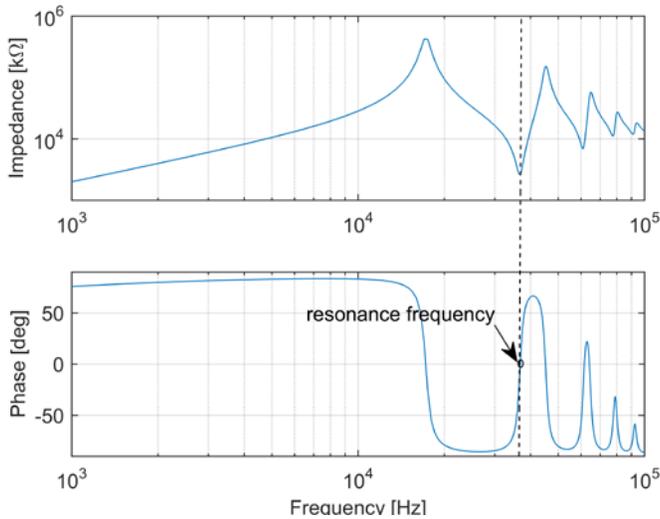
Figure 6. Harmonic terminal impedance of the studied transformer winding with the most severe resonance frequency; amplitude characteristic (upper trace) and phase characteristic (lower trace).
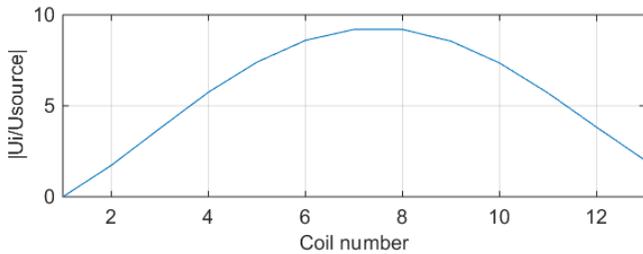
Figure 7. Computed amplification factors for the denoted resonance frequency.
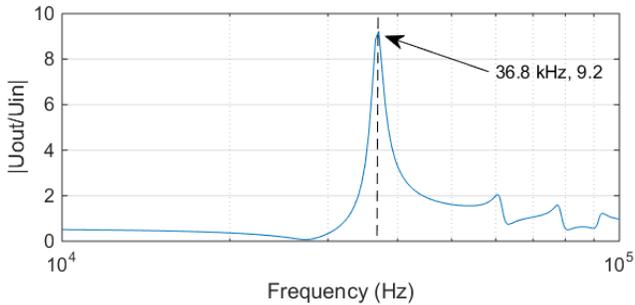
Figure 8. Computed amplification factor for coil 7.

The amplification factor of coil 7 is represented in Figure 8. It can be seen that at 36.8kHz the voltage may rise up to 9.2 pu.

In order to observe the variation of the voltages in different coils, the transformer is excited by a sinusoidal pulse with duration of different periods and frequency equal to the observed resonance frequency. Figures 9 through 11 shows the variation of voltages in some coils. Figure 9 corresponds to a voltage excitation with two periods. It can be seen that the maximum voltage in this case is about 2.3 times higher than the source voltage applied to the transformer.
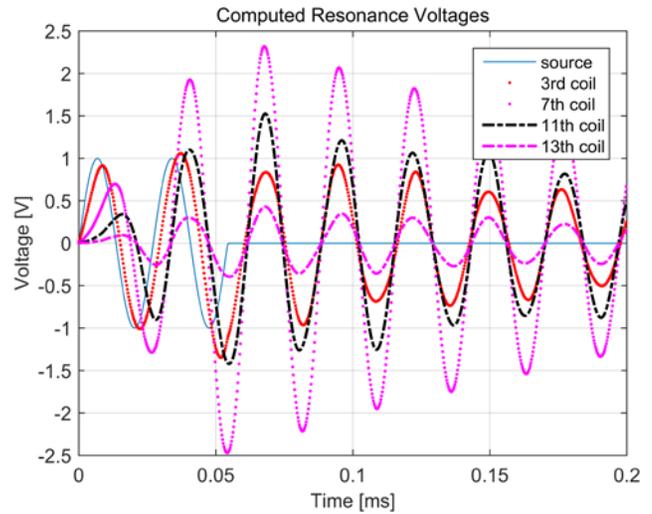
Figure 9. Computed resonance voltages for an excitation with 2 periods.
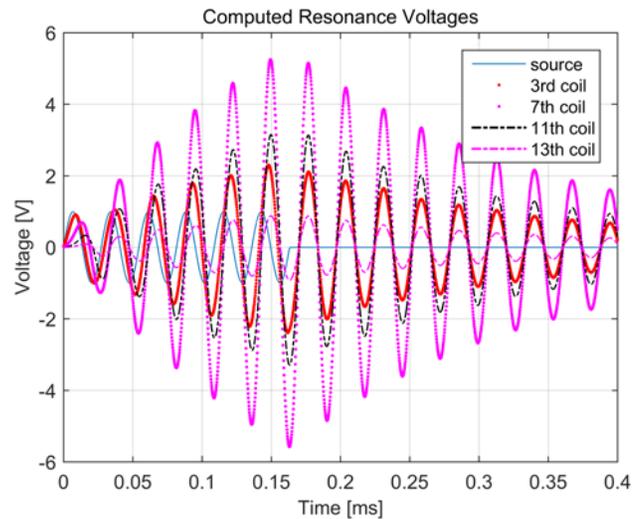
Figure 10. Computed resonance voltages for an excitation with 6 periods.
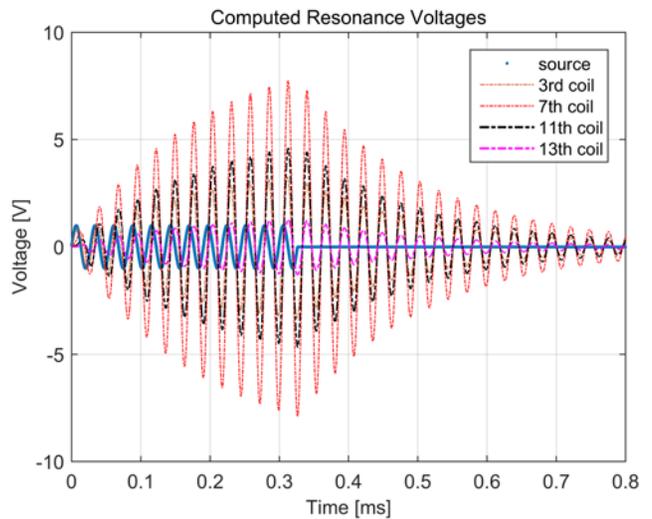
Figure 11. Computed resonance voltages for an excitation with 12 periods.

Analogously, Figures 10 and 11 show the voltage variation when the transformer is excited with the same pulse in amplitude and frequency, but with different duration. In Figure 10, the excitation pulse contains 6 periods whilst in Figure 11,

it is with duration of 12 periods. The difference in the results of the studied cases can be observed in the amplitude of the maximum overvoltages. With other words, when the pulse duration increases, the amplitude of the resonance voltages increase accordingly. Appendix II summarizes voltages in coil 7 for a source voltage with 12 periods and 24 periods respectively.

Maximum resonance overvoltages for different pulse durations are summarized in Figure 12. For the studied transformer, the voltage distribution was also computed during 50 Hz excitation. Voltages are linearly distributed starting at 1 pu in the first coil with a gradual decrease toward the receiving end of the winding. On the other hand, it can be seen that the maximum overvoltages gradually increase by the increase of the pulse duration. The non-linear voltage distribution in this case is obvious.
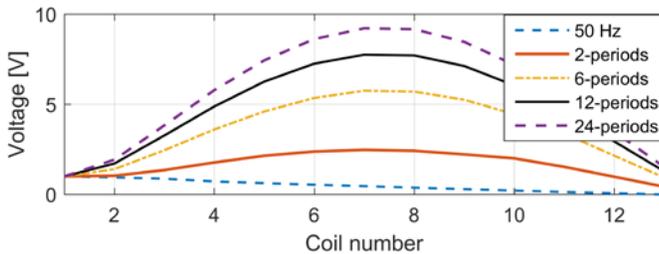
Figure 12. Voltage distribution during resonance for different duration of the excitation compared with to voltage distribution during normal operation (50 Hz).

This means that during resonance, it is important how long the transformer is exposed to resonance. For excitations with short duration, the released amount of energy is lower than that during excitation with longer duration. Finally, when the duration of the impulse is long enough, the maximum overvoltage will be equal to the computed amplification factor. From Figure 12, it can be seen that voltage in coil 7 becomes equal to the maximum amplification factor 9.2 when the excitation impulse has 24 periods, which also can be seen from Figure 8.

V. DISCUSSION

The computed results show that the resonance may lead to severe overvoltages, which are several and even tens of times higher in amplitude than the applied voltages at the transformer terminal. In [4], a detailed analysis was performed in which transformer reaction to overvoltages was tested upon different network conditions complying different loads and cable lengths during transformer energization and de-energization. The severity factor [4],[9],[10] was estimated based on an envelope designed by the switching impulse level and lightning impulse level. From the measurement and simulation, it was found that the overvoltages were not that high and the transformer may not face difficulties. The analyzed overvoltages resulted due to multiple restrikes and prestrikes when switching the transformer with a vacuum circuit breaker. It is obvious that an oscillation with the most severe resonance frequency did not take place. The type of the

model that can be used for this purpose depends on the frequency range. In case, when frequency losses are well estimated and can be represented with constant parameters, an EMT-based model can also be used successfully. For a broad frequency range, above 100 kHz, proximity losses heavily vary with the frequency so that computation difficulties may be faced. In such case, it is strongly recommended to make use of an analysis in which frequency dependent parameters due to variable losses, skin effect and dielectric permittivity are computed within broad frequency range.

In general, networks which are vulnerable to harmonics may be permanently exposed to high overvoltages. Besides, it is useful to investigate the interaction of the transformer with the network and see if there are circumstances so that the transformer may enter in resonance with the surrounding network. Possible cases may be lightning in the surrounding of a high power transformer, transformer energization (prestrike effect) or transformer de-energization. The latter, may result in sever multiple restrikes, which may lead to oscillations with different frequencies. In the past work [5], it was shown that the oscillations of multiple restrikes are not only dependent on the circuit breaker parameters but also on the connection between the transformer and the circuit breaker. In case of a cable connection, cable resonance frequencies may also influence the total resonance frequency of the system cable – transformer. This is subject of future investigation.

Besides, high power, high voltage transformers may have more resonance frequencies up to 100 kHz than medium voltage transformers, hence the likelihood a resonance to occur is higher. Another point of interest for the future will be the overvoltage level during excitation with a resonant frequency oscillation that is chopped. This may result in higher overvoltage and comprehensive analysis will be needed to see if the overvoltage amplitude may exceed the insulation level.

VI. CONCLUSIONS

The paper presents a comprehensive and detailed analysis of resonance effects in transformers. The analysis is performed on only one transformer phase, however, the approach is generally applicable for any transformer as long as the inductance and capacitance matrix as well as losses are accurately determined. It is valid for multi-winding multi-phase transformers with any type of winding. Z matrix of transformer windings contains all the information about the voltage and current distributions in the winding.

The transformer saturation in this case is not taken into account. However, since the impedances are computed in frequency domain, the influence of the core can also be taken into account. Anyhow, experience shows that the core has limited influence up to several tens of kilohertz. This has been validated by measurements on open and short circuited secondary winding of the transformer [5]. The applied parameters, which are explained in more detail in [4] are computed in a way that the flux does not penetrate the core. Experience and previous work reveals that above several tens of kilohertz this is justified. In this work, it is shown that the

voltage distribution for existing resonance frequencies can be determined by computing the amplification factor based on the provided characteristics. Here, only one resonance frequency was analyzed. Voltage distributions for different resonance frequencies can be calculated in the same way. This analysis has also shown that another crucial factor, which influences overvoltage amplitude is the excitation duration. When a transformer is exposed to resonance oscillations for a longer time, the value of the maximum amplification factor of some coil can be reached.

Finally, lossy frequency dependent inductances obtained by Wilcox's approach [11] can be used to represent transformer frequency-dependent losses and inductances. On one hand, the representation of these matrices in EMTP-based environment is possible by making use of constant parameters for the resistances and inductances. On the other hand, this is not fully accurate since frequency-dependency is not taken into account. One solution regarding this issue is to define the validation of these parameters for particular frequency range and make use of such model for particular bandwidth.

VII. APPENDIX I

Data for the transformer test coil: L_{11}=28.988 mH; M_{12}=13.537 mH; M_{13}=6.231 mH; M_{14}=3.379 mH; M_{15}=1.987 mH; M_{16}=1.242 mH; M_{17}=0.817 mH; M_{18}=0.56 mH; M_{19}=0.398 mH; M_{110}=0.292 mH; C_g=850 pF; C_s=3.4 pF; R_g=2.1e11 Ω; R_s =1.65e5 Ω; r=22.6 Ω; where C_s is a series capacitance between coils, C_g is a capacitance between node to ground. $1/R_s$ and $1/R_g$ are series and shunt admittances respectively used to build the admittance matrix $\mathbf{G}$, whilst r is the coil resistance of the coils. $\mathbf{C}$-matrix is built in the following way: Diagonal elements: sum of all capacitors connected to a particular node i; Off-diagonal elements: a capacitance with negative sign connected between node i and node j. In case when there is no capacitance between node i and node j, the element is zero. The admittance matrix $\mathbf{G}$ is formed in the same way as the $\mathbf{C}$-matrix. Coil resistances are included in the inductance matrix $\mathbf{L}$ only in the diagonal elements.

VIII. APPENDIX II

Comparison of resonance overvoltages with an excitation of 12 and 24 periods respectively.
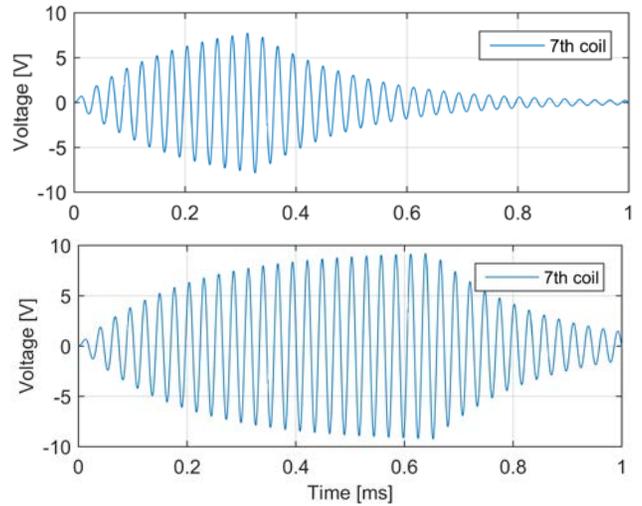
Figure I. Resonance voltage in the 7th coil for a source with 12 periods (upper) graph and 24 periods (lower graph).

IX. REFERENCES

[1] R. C. Degeneff: "A General Method for Determining Resonances in Transformer Windings", *IEEE Trans. Power App. Syst.*, PAS-76, no. 2, March/April 1977, pp. 423–430.

[2] B. Gustavsen, "Computer code for rational approximation of frequency dependent admittance matrices," *IEEE Trans. Power Del.*, Vol. 17, No. 4, pp. 1093–1098, Oct. 2002.

[3] D Filipović-Grčić, B Filipović-Grčić, I Uglešić: High-Frequency Model of the Power Transformer Based on Frequency-Response Measurements, *IEEE Transactions on Power Delivery* Vol. 30, No. 1, February 2015, pp. 34-42.

[4] A. Theocharis, M. Popov, R. Seibold, S. Voss and M. Eiselt: "Analysis of Switching Effects of Vacuum Circuit Breaker on Dry-Type Foil-Winding Transformers Validated by Experiments", *IEEE Transactions on Power Delivery*, Vol. 30 , No. 1, February 2015, pp. 351-259.

[5] M. Popov, R.P.P. Smeets, L. van der Sluis, H. de Herdt and J. Declercq: Experimental and Theoretical Analysis of Vacuum Circuit Breaker Prestrike Effect on a Transformer, *IEEE Transactions on Power Delivery*, Vol. 24, No. 3, July 2009, pp. 1266-1274.

[6] M. Popov, L. van der Sluis, G.C. Paap, H. de Herdt: "Computation of Very Fast Transient Overvoltages in Transformer Windings", *IEEE Transactions on Power Delivery*, Vol. 18, Issue 4, pp. 1268-1274, 2003.

[7] Pt. Bickford J.P., Mullineux N., Reed J.R.: "Computation of Power System Transients", IEE, Peter Peregrinus Ltd., 1976, ISBN 0901223859.

[8] A. Theocharis, M. Popov: "Modeling of Foil-type Transformer Windings for Computation of Terminal Impedance and Internal Voltage Propagation", *Proceedings of IET Electrical Power Applications*, Vol. 9, Issue 2, pp. 128-137, 2015.

[9] JWG A2/C4.39, Electrical Transient Interactions between Transformers and the Power System, *ELECTRA* No. 273-April 2014, pp. 97-103.

[10] C. Álvarez-Mariño, X. M. Lopez-Fernandez, A. J. M. Jácomo-Ramos, R. A. F. Castro-Lopes, and J. M. Duarte-Couto, "Time domain severity factor (TDSF): Induced transient voltage between transformer and vacuum circuit breakers," *Int. J. Comput. Math. Elect. Electron. Eng.*, Vol. 31, No. 2, pp. 670–681, 2012.

[11] D.J. Wilcox,, W.G. Hurley, and M. Conlon: 'Calculation of self and mutual impedances between sections of transformer coils', IEE Proc. C, 1989, 136, (5), pp. 308–314.